Primary Formation Dynamics of Peroxynitrite Following Photolysis of Nitrate

Jan Thøgersen, Ane Gadegaard, Jakob Nielsen, Svend Knak Jensen, Christian Petersen,[†] and Søren R. Keiding*

Department of Chemistry, University of Aarhus, Langelandsgade 140, DK-8000 Aarhus C, Denmark

Received: July 6, 2009; Revised Manuscript Received: August 12, 2009

The photolysis of nitrate, NO_3^-, in D_2O solution has been investigated by femtosecond infrared spectroscopy. In accordance with previous investigations, we observe that the peroxynitrite ion, $ONOO^-$, is the dominant photochemical product following the excitation of nitrate at 200 nm. Moreover, we are able to identify the cis/trans isomers of peroxynitrite and the dynamics of their formation in solution. We observe that the *trans*-$ONOO^-$ isomer is formed directly and solely from the excited NO_3^- ion within the first two picoseconds after excitation. Subsequently, about half of the *trans*-$ONOO^-$ isomerizes to *cis*-$ONOO^-$ in 25 ps; thereafter, the ratio between the two isomers remains constant for the 300 ps duration of the experiment. The observed vibrational frequencies of the terminal O═N bonds are at 1515 and 1580 cm^{-1} for *trans*- and *cis*-peroxynitrite, respectively. The detailed analysis of the infrared bands of *cis*- and *trans*-peroxynitrite is facilitated by electronic structure calculations on the conformers in a cluster of 11 D_2O molecules and by steady-state infrared spectroscopy of $ONOO^-$ in D_2O. In addition to the formation of $ONOO^-$, the experiments also reveal a slow ~50 ps formation of NO_2 following the photolysis of nitrate.

Introduction

This work describes one of the most common photochemical transformations in aqueous environments: the photoisomerization of the aqueous nitrate into peroxynitrite and the subsequent isomerization of *trans*-peroxynitrite into *cis*-peroxynitrite.[1] The nitrate−peroxynitrite system has thus been studied in great detail as a model system for aqueous chemical reactions[2−10] because it displays all key concepts in aqueous chemistry: charge stabilization, electron detachment, high mobility, contact pairs, solvent caging, and energy dissipation through the hydrogen bond network. In addition, peroxynitrite plays a very important role as a biochemical oxidant and nitrating agent formed in vivo from nitric oxide, NO, and superoxide, O_2^-.[11−15] The presence of elevated concentrations of peroxynitrite has been linked to a broad range of cardiovascular and other pathologies. Peroxynitrite leads to oxidative stress in many organisms and inflicts damage to blood vessels, skin, heart, lung, kidney, and brain. Consequently, there are numerous papers published on the fundamental properties of the nitrate−peroxynitrite system, and, in particular, on the biomedical implications of peroxynitrite. Contrary to most of the previous work on the nitrate−peroxynitrite system, the work presented here is performed with femtosecond time resolution. Apart from the deservedly celebrated possibility of observing chemical transformation in real time, the short time resolution actually presents another advantage of similar proportions: The diffusion coefficient of a small molecule in water is typically $D \approx 2 \times 10^{-9}$ m^2 s^{-1} (= 0.2 $Å^2$ ps^{-1}), and the diffusion length is $L_D = (6Dt)^{1/2}$. Consequently, the volume of the solution covered by the diffusing molecules is very small on femto- and picosecond time scales. If, for example, an excited NO_3^- molecule were to encounter a molecule other than water, in 50 ps, the concentration of this molecule should exceed 1 M. Therefore, the time resolution ensures that only the primary photodynamics are investigated and that secondary reactions can safely be neglected. For the nitrate−peroxynitrite system, in particular, the ability to perform a "collision and impurity free" experiment is very important because of the high reactivity of peroxynitrite.[2]

We have previously investigated the nitrate−peroxynitrite system with femtosecond time resolution using ultraviolet laser pulses. Unfortunately, the specificity of the ultraviolet absorption spectra of the involved photoproducts is low because they all have rather broad and featureless absorption spectra in the range between 200 and 300 nm. Therefore, although we could determine the primary quantum yields of peroxynitrite from the photolysis of NO_3^-, we could not directly determine which of the isomers of peroxynitrite was formed. In this work, we extend our previous studies of the nitrate−peroxynitrite system by utilizing femtosecond transient absorption spectroscopy in the infrared spectral region. This allows us to determine the distribution of peroxynitrite isomers formed after the excitation of nitrate. In our previous work,[5] we assigned the transient UV spectrum of peroxynitrite solely to the cis isomer, and this was recently questioned by Rabani et al.,[6] who suggested that the trans isomer should also be present after photolysis of nitrate. Using Raman spectroscopy, Tsai et al. have found that only the cis isomer is observed under ambient conditions.[16] Using femtosecond IR transient absorption spectroscopy, we can distinguish the trans and cis isomers and thus reveal how they are generated from nitrate and their rate of conversion. Furthermore, our experiments also reveal the slow (50 ps) formation of NO_2 following the photolysis of nitrate. This observation resolves the current uncertainty[6] concerning the third channel in the primary photolysis of nitrate. Internal conversion of excited nitrate and isomerization into peroxynitrite constitutes ~75−85% of the yield following the photolysis of nitrate, and from our data, we see that the formation of NO_2 constitutes the last ~15−25%.

* Corresponding author. E-mail: keiding@chem.au.dk. Tel: +45 2899 2061/+45 8942 3861. Fax: +45 8618 6199.

[†] Present address: FOM Institute for Atomic and Molecular Physics (AMOLF), P.O. Box 41883, 1009 DB Amsterdam, The Netherlands.

10.1021/jp906354c CCC: $40.75
Published on Web 09/08/2009

TABLE 1: Vibration Frequencies and Intensities[a]

	ω_{calcd} (cm^{-1})	$0.9664 \times \omega_{calcd}$[b]	ω_{obsd} (cm^{-1})	I_{calcd} (km/mol)
NO_3^-, 11 D_2O	1417 ± 12	1369	1370[c]/1350[d]	421 ± 46
	1499 ± 14	1449	1400	439 ± 46
NO_3^-, K^+, 11 D_2O	1425 ± 19	1377	1370	442 ± 77
	1504 ± 22	1453	1400	391 ± 46
cis-$ONOO^-$, 11 D_2O	1701 ± 18	1644	1560[c]/1564[d]	321 ± 33
			1580[e]	
trans-$ONOO^-$, 11 D_2O	1605 ± 37	1551	1515[e]	232 ± 39
NO_2, 11 D_2O	1726 ± 3	1668	1610[e]	333 ± 23

[a] ω_{calcd} is the harmonic normal mode frequency with a dominant contribution from the terminal N=O vibration calculated at the B3LYP/6-31G(d) level of theory. The two frequencies in the case of NO_3^-(aq), 11 D_2O correspond to the highest E' frequency, ν_3 of NO_3^-(aq). I_{calcd} is the calculated intensity of the corresponding transition. ω_{obsd} is the experimental transition frequency assigned to scaled calculated frequency using the scale factor of 0.9664.[19] [b] Ref 19. [c] This work, pD > 11. [d] Ref 16. [e] This work, pD = 7.

Experimental and Theoretical Methods

The laser pulses are produced by an amplified titanium−sapphire laser system. The laser pulses are 100 fs long and have a center wavelength of 800 nm and pulse energy of 1 mJ. The laser beam is divided into two equally powerful beams. The beam of 200 nm excitation pulses is generated by frequency doubling and sum-frequency-mixing the 800 nm laser pulses in three β-barium borate (BBO) crystals. The resulting pump beam is focused onto the sample by a concave mirror. The beam of probe pulses is generated by difference frequency mixing the signal and idler pulses from an optical parametric amplifier, which is pumped by the second beam from the titanium−sapphire laser system. The probe beam is divided into a signal and a reference beam. The signal beam is probing the sample inside the volume excited by the pump pulse, whereas the reference beam bypasses the sample. The signal and reference beams are subsequently sent through a grating spectrometer and measured by a 2×32 channels cooled dual-array HgCdTe detector. The accuracy of the energy scale calibration is ± 10 cm^{-1}, corresponding roughly to 1 pixel in the HgCdTe detector.

The sample consists of 0.07 M aqueous KNO_3. Thin liquid films of the samples are suspended in a constant flow between two parallel, 50 μm thick titanium wires separated by 4 mm.[17] No sample degradation is observed in the measurements, but to avoid the potential buildup of photoproducts, we replace the sample on a daily basis. This also reduces the accumulation of HDO resulting from the gradual exchange of D_2O with HDO caused by the absorption of H_2O by the thin liquid film and subsequent H−D exchange in the sample reservoir. The measurements presented below are taken with the polarizations of the excitation and probe beams oriented at 90° with respect to each other. This reduces the strong coherence spike at zero delay present with collinear polarizations of the two beams.

To facilitate the experimental identification of the various reactants and products, we performed electron structure calculations on the species solvated by 11 water molecules (D_2O) using the Gaussian03 software.[18] A potential minimum was found that allows the calculation of the harmonic vibration frequencies for normal and heavy water. The chosen level of theory is the B3LYP implementation of the density functional theory with the basis set 6-31G(d). Inspection of the various frequencies showed that the normal mode with a dominant contribution from the terminal N=O stretch was a useful fingerprint in D_2O because its absorption is well separated from other bands. When NO_3^- is converted into $ONOO^-$, the rearrangement of solvent molecules around the anion changes because of differences in geometry and charge distribution. To obtain some measure for the sensitivity of the frequencies to the solvent rearrangement, we have repeated the calculations for a number of different configurations. The average value and the rms uncertainty are listed in Table 1. The calculated vibrational frequencies were multiplied with a scaling factor of 0.9664 before comparison with the experimental transition frequencies.[19]

The geometry of the nitrate anion requires a comment. The isolated ion has a three-fold axis of symmetry, and the considered N−O stretch vibration (E') is two-fold degenerate. In the solution, this symmetry is broken and the degeneracy is lifted, causing the vibrational line to split into two.[20] In nitrate salts, the magnitude of the splitting depends on the counterion.[21] We have also calculated the N−O stretch frequency for clusters that include the potassium ion. (See Table 1.) The calculated splitting of about 80 cm^{-1} is roughly the same in the three cases, confirming that the splitting observed in NO_3^-(aq) is caused by the solvent. Table 1 also shows that the N=O bands in *cis*- and *trans*-$ONOO^-$ are separated by about 100 cm^{-1}, with the cis isomer assigned to the highest vibrational transition frequency, which is in agreement with most previous studies.[22−24] For the potassium and hydrogen salts of peroxynitrite in matrices, this tendency is reversed.[25,26]

To obtain the steady-state infrared spectrum of peroxynitrite, we synthesized peroxynitrite. The setup for the synthesis of peroxynitrite in H_2O was as described by Robinson and Beckman.[27] We note that by lowering the temperature to ~5 °C, the yields are increased. Using the UV extinction coefficient of $ONOO^-$ ($\varepsilon = 1670$ M^{-1} cm^{-1} at $\lambda = 302$ nm),[28] we determined the concentration of $ONOO^-$ to be 0.3 M. The bending mode of liquid H_2O is at 1644 cm^{-1} and thus precludes the identification of typical N=O vibrations in the range from 1400 to 1700 cm^{-1}. The D_2O bending frequency is at 1210 cm^{-1}. Therefore, to facilitate the observation of the vibrational transition frequencies in the infrared, we removed the H_2O solvent by repeated vacuum distillation (35 °C at 20 mbar) and addition of D_2O to the solution. After three to four cycles, most H_2O was either removed or exchanged to form HDO. Interestingly, we were not able to synthesize any $ONOO^-$ using the procedure described by Robinson and Beckmann[27] using fully deuterated solvents and reagents.

The observed infrared spectrum of $ONOO^-$ is shown in Figure 1. A drop of the solution is placed between two CaF_2 windows to obtain a sample thickness of ~5−10 μm. The cutoff observed below 1000 cm^{-1} is caused by the CaF_2 window material. The D_2O bending mode is observable at 1210 cm^{-1}, but the corresponding bending modes of H_2O and HDO at 1644 and 1460 cm^{-1} are not observed. The broad double peak at 1370/1400 cm^{-1} corresponds to nitrate, which is a known byproduct of the synthesis of $ONOO^-$. Finally, we assign the line at 1560 cm^{-1} to *cis*-$ONOO^-$. The solution of $ONOO^-$ is strongly basic (pD > 11) to stabilize the $ONOO^-$, and we believe that the slight

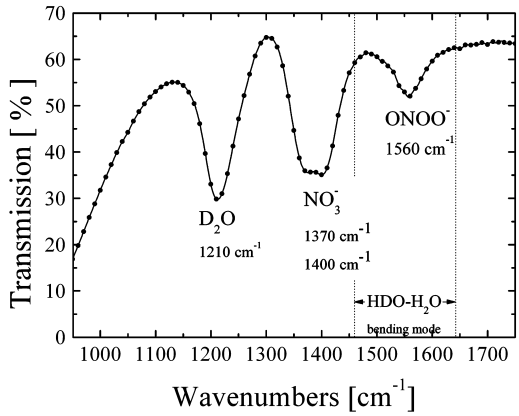

Figure 1. Infrared absorption spectrum of $ONOO^-$ in D_2O. The sample is contained between two CaF_2 windows spaced by $\sim$5−10 μm. The low frequency cutoff is caused by the windows. The NO_3^- signal is a byproduct of the synthesis. The H_2O solvent was replaced by D_2O by vacuum distillation, and no traces of either HDO or H_2O are observed in the spectrum.

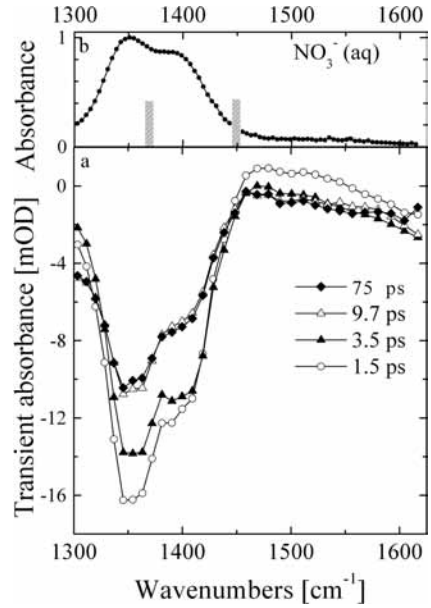

Figure 2. (a) Transient infrared absorption following the photolysis at 200 nm of 0.07 M NO_3^- in D_2O. The transient absorption reveals the strong bleaching of the nitrate vibrational transition at 1350 and 1400 cm^{-1} and induced absorption at higher frequencies. (b) Infrared absorption frequencies of NO_3^- in H_2O. The two bars indicate the position of the calculated frequencies. The bleaching in Figure 2a recovers in a few picoseconds, and the similar line shapes in the transient (a) and steady state (b) spectra are indicative of vibrational relaxation not involving the N═O stretching vibrations.

difference between the observed *cis*-$ONOO^-$ line position at 1580 cm^{-1} in the femtosecond experiments (pD $\approx$ 7) and 1564 cm^{-1} in Raman and 1560 cm^{-1} in infrared absorption (pD > 11) is caused by the difference in basicity.

Results

We have divided the presentation of the results into four subsections. First, we briefly recapitulate the results of the UV pump UV probe experiments. Then, we address the presence of the strong background signal from the water solvent, and in the last sections, we describe the assignment of the transient infrared spectrum and the temporal dynamics of the observed infrared peaks.

In our previous work,[5] we have shown that when photolyzed at 200 nm, 48% of the nitrate molecules will form peroxynitrite, 44% will return to the ground state of nitrate through fast internal conversion, whereas the remaining 8% was ascribed to a solvent separated pair of $[O_2 + NO]^-$, where the exact location of the negative charge could not be determined. The formation of these reaction products is in all three cases observed within the 300 fs time resolution of the experiment. The nitrate, formed through internal conversion, is vibrationally hot, and within 2 ps, this excess energy relaxes and the NO_3^- molecule is again in the electronic and vibrational ground state.

$$NO_3^- + \hbar\omega\ (200\ \text{nm}) \xrightarrow{k\ \geq\ 3\ \text{ps}^{-1}} ONOO^- \quad (48\%)$$

$$\xrightarrow{k\ \geq\ 3\ \text{ps}^{-1}} [NO_3^-]^{\otimes} \xrightarrow{k_{\text{vib rel}}\ \approx\ 0.5\ \text{ps}^{-1}} NO_3^- \quad (44\%) \qquad (1)$$

$$\xrightarrow{k\ \geq\ 3\ \text{ps}^{-1}} [NO + O_2]^- \quad (8\%)$$

In this work, we focus on the product channel where peroxynitrite is formed, and we use femtosecond infrared pulses to follow the reaction products.

Infrared spectroscopy of aqueous systems, in particular, with femtosecond time resolution is inherently difficult. First of all, the infrared absorption of water is very strong and spreads over most of the infrared region with just a few narrow windows with low absorption. Second, the infrared spectrum of water is very temperature-dependent.[29,30] When working in pump−probe mode, where a strong pump initiates a chemical change, there will be a large transient signal due to water that tends to obscure signals from solute molecules. This is, in particular, the case when the solute is hydrogen bonded to the water solvent. To circumvent these challenges, we use heavy water, D_2O, which is relatively transparent in the range from 1300 to 1900 cm^{-1}. Furthermore, we use a thin wire-guided film of liquid water with a thickness between 10 and 20 μm to allow for sufficient transmission of the infrared probe. Finally, we have conducted a series of control experiments using nitrite, NO_2^- in H_2O and D_2O and used the results to estimate the background response from the water solvent. However, true background subtraction cannot be obtained because the specific hydrogen (deuterium) bonding of both nitrite and nitrate is different.

Figure 2a shows the transient infrared absorption in the region from 1300 to 1600 cm^{-1} following photolysis of a 0.07 M solution of NO_3^- at λ = 200 nm. Figure 2b shows the infrared absorption of NO_3^- in aqueous solution obtained from an FTIR spectrometer. The characteristic double peak in Figure 2b comes from the degenerate ν_3 vibrations where the degeneracy has been lifted by interaction with the solvent.[8,20,21] The two gray bars are the calculated vibrational frequencies listed in Table 1 for the nitrate molecules microsolvated by 11 D_2O molecules. The transient signal in Figure 2a shows a strong bleaching caused by the removal of nitrate molecules by the pump pulse. The nitrate signal recovers during the first 10 ps because of internal conversion and vibrational relaxation according to the reaction schemes in eq 1. The line shape of the transient absorption is very similar to that of the absorption spectrum in Figure 2b, indicating a very fast vibrational relaxation mostly taking place through low-frequency vibrations and not the N═O stretching

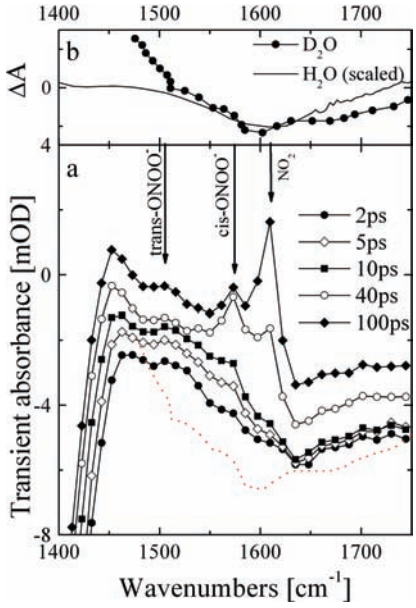

Figure 3. (a) Transient infrared absorption following the photolysis at 200 nm of 0.07 M NO_3^- in D_2O at selected delays showing the absorption lines of *trans*-$ONOO^-$, *cis*-$ONOO^-$, and NO_2 and the high frequency wing of the NO_3^- bleaching. The data were offset for clarity. The red dotted line is the background signal from the thermally excited D_2O solvent obtained from the measurements of the solvent response following the photolysis of NO_2^- shown in part b. (b) Background obtained from the photolysis of nitrite (NO_2^-) in both D_2O and H_2O, where results from H_2O was frequency scaled by $\sqrt{2}$.

modes. This is in good agreement with the notion that the excited state populated in nitrate by the 200 nm pump pulse has a pyramidal geometry giving rise to strong excitation of bending modes upon internal conversion to the planar nitrate ground state.

We now turn our attention to the transient infrared spectrum of peroxynitrite observed following the photolysis of nitrate at 200 nm. Guided by the infrared spectrum in Figure 1, the Raman spectra of peroxynitrite,[16] showing a broad absorption line at 1564 cm^{-1}, and our calculations of the microsolvated peroxynitrite isomers listed in Table 1, we focus our attention on the transient spectrum in the range from 1500 to 1700 cm^{-1} shown in Figure 3a. In Figure 3b we also show the transient spectrum observed 50 ps after the photolysis of nitrite.[30] In nitrite, most of the transient absorption in this region can be assigned to the solvent alone, and the spectrum in Figure 3b can thus serve as an approximate background spectrum for the photolysis of nitrate. We show both the spectrum obtained in D_2O (filled circles) and the spectrum obtained in H_2O (full line). The H_2O spectrum was spectrally shifted by dividing the frequency axis with $\sqrt{2}$. In D_2O, the dominant solvent mode in this frequency range is the combination band containing the bending mode and the low-frequency libration mode. The factor $\sqrt{2}$ thus approximately shifts the H_2O spectrum to the corresponding position in D_2O. The overall shapes of the background spectra are similar, reflecting a temperature increase in the solvent causing a red shift of the combination band.[30] The transient absorption of the nitrate−peroxynitrite system is shown in Figure 3a. At the lowest frequencies, we observe the nitrate bleaching also shown in Figure 2a, and at higher frequencies, we observe a modulated signal caused by the combined signals from the solvent background and the transient signal from the photolysis of nitrate. We have measured the transient signals to a delay of 300 ps and show only selected time delays in Figure 3a.

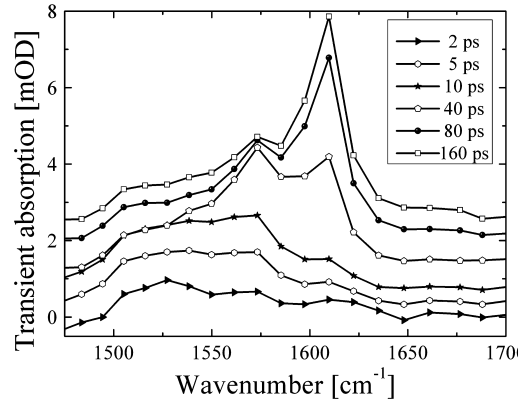

Figure 4. Transient infrared spectra obtained by subtracting the D_2O background obtained from Figure 3b. Amplitude scaling of the background was obtained from the frequency range between 1650 and 1700 cm^{-1}, where only the solvent contributes to the signal. At short delays, the broad *trans*-$ONOO^-$ absorption from 1500 to 1550 cm^{-1} dominates. After 10 ps, the *cis*-$ONOO^-$ absorption appears at 1580 cm^{-1}, and half of the *trans*-$ONOO^-$ absorption remains at 1515 cm^{-1}. The absorption at 1610 cm^{-1}, assigned to NO_2, rises with a time constant of ~50 ps and remains constant after 80 ps.

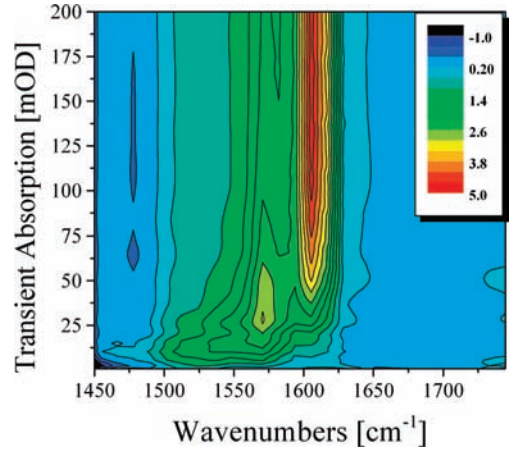

Figure 5. 2D representation of the full set of time delay versus probe frequency. The estimated solvent response from D_2O was subtracted from the data. The experimental data show the initial broad features assigned to *trans*-$ONOO^-$ gradually relaxing to the *trans*- and *cis*-$ONOO^-$ absorption at 1515 and 1580 cm^{-1}. Isolated from these events, the NO_2 signal at 1610 cm^{-1} appears on a 50 ps time scale.

To facilitate the analysis and assignment of infrared spectral features to *cis*- and *trans*-peroxynitrite, we show in Figure 4 the transient signals at five delay times from 2 to 100 ps. At each delay, we have normalized the background estimated from Figure 3b to give a "zero baseline" of the residual transient absorption. We note that in the region above 1675 cm^{-1}, the time dependence of the transient absorption in both nitrite and nitrate is similar, reflecting the same solvent response. The transient signals are vertically displaced for visual clarity. We observe three distinct spectral features in Figure 4. There are two absorption lines at 1515 and 1580 cm^{-1}, which we assign to *trans*- and *cis*-peroxynitrite, respectively, guided by the IR and Raman spectra and the calculated vibrational frequencies. In addition, we observe at long delays appearing after ~50 ps a prominent infrared peak at 1610 cm^{-1}. We also observe this peak in the photolysis/photodetachment of nitrite and assign it to NO_2. The full set of transient absorption at all probe frequencies is shown in a 2D plot in Figure 5. As in Figure 4, the background caused by the heating and subsequent thermalization of the solvent has been subtracted.

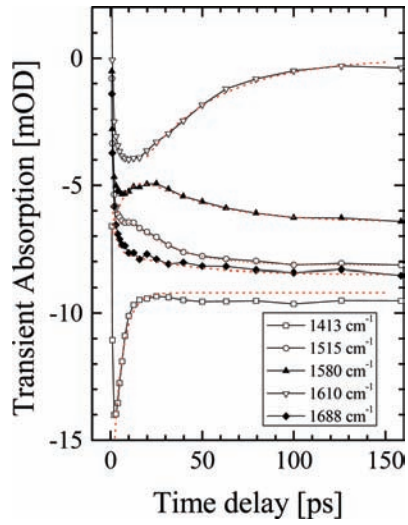

Figure 6. Transient absorption traces at selected probe frequencies showing the dynamics of the solvent (1688 cm^{-1}), NO_2 (1610 cm^{-1}), *cis*-$ONOO^-$ (1580 cm^{-1}), and *trans*-$ONOO^-$ (1515 cm^{-1}) and the bleaching of NO_3^- at 1413 cm^{-1}. The data are shifted for clarity. The estimated solvent background was not subtracted from the data.

In Figure 6, we show the time dependence of the transient absorption at five selected probe frequencies close to representative transitions: the solvent response at 1688 cm^{-1}, the nitrate bleach at 1413 cm^{-1}, the absorption signals corresponding to *cis*- and *trans*-peroxynitrite at 1562 and 1527 cm^{-1}, and the 1610 cm^{-1} feature assigned to NO_2. We have displaced the five curves slightly to emphasize visually their time dependencies. The trace at 1688 cm^{-1} is dominated by the combination band of water (D_2O) composed of the bending mode and the librational band. Following the photolysis of nitrate, the solvent heats up, causing the combination band to red shift, which gives rise to a strong negative transient absorption (bleaching) at the probe frequencies from 1625 to 1740 cm^{-1} in Figure 5.[30] The time dependence of the solvent signal reflects the dissipation of heat from the reaction site and is well represented by a double exponential decay with decay times of 1.8 and 36 ps. This temporal behavior of the signal at 1688 cm^{-1} is similar to the transient absorption observed in nitrite at probe frequencies far from nitrite resonances.[30] We know from previous work that the spectral profile of the solvent relaxation is unchanged after ~2 ps, so any time dependence different from the double exponential decay at 1688 cm^{-1} is indicative of the dynamics of the reaction products.

The 1515 cm^{-1} signal, corresponding to the *trans*-$ONOO^-$ peak, appears within the time resolution of the experiment. In Figures 4 and 5, it is seen that the *trans*-$ONOO^-$ absorption at short delays is broader and shifted to lower wavenumbers. The signal gradually blue shifts and decays. The time constant for this decay is difficult to entangle from the strong solvent response, but we estimate that the *trans*-$ONOO^-$ absorption decays to half of its initial value in 25 ps. The decay of the *trans*-$ONOO^-$ absorption is followed by a similar rise of the *cis*-$ONOO^-$ absorption at 1580 cm^{-1}. If the decay times of the solvent are taken into account, then the signals from *trans*- and *cis*-$ONOO^-$ exhibit the same decay and risetime of about 25 ps. After 50 ps, both the *trans*- and *cis*-$ONOO^-$ signals remain largely unchanged. We estimate that about half of the *trans*-$ONOO^-$ isomerizes to *cis*-$ONOO^-$ and that the initial concentration of the *cis*-$ONOO^-$ isomer is close to zero. The estimate is based on the calculated intensities, shown in Table 1, for the infrared transitions in the cis and trans isomers. This indicates that only the *trans*-$ONOO^-$ isomer is formed directly from the photoexcited nitrate molecules. Referring to the our previous study of the UV-pump UV probe experiments,[5] we note that the UV absorption spectra of *cis*- and *trans*-$ONOO^-$ are very similar. The observation of solely *trans*-$ONOO^-$ immediately after photolysis of nitrate and the gradual conversion of half of the molecules into *cis*-$ONOO^-$ is thus in accordance with our observations in the UV region. From the previous experiments,[5] we know that the concentration of peroxynitrite at pH ~7 is constant from just after the photolysis pulse up to the longest delays measured (300 ps). The assignment of *trans*- and *cis*-$ONOO^-$ at 1515 and 1580 cm^{-1} is further corroborated by lowering the pH (pD) of the solution and monitoring the decay of the amplitudes of the 1515 and 1580 cm^{-1} signals because of diffusive protonation of $ONOO^-$.[4] Comparing the bleaching of the NO_3^- signal at 1350 and 1400 cm^{-1} with the induced absorption of $ONOO^-$ and taking into account the line strength calculated also provides a rough verification of the quantum yields previously measured in the UV region.[5]

Discussion

The infrared frequencies pertaining to the terminal O═N bond in both *cis*- and *trans*-peroxynitrite is central to this work. Experimentally, the only observation of peroxynitrite vibrational frequencies in aqueous phase is the Raman spectra of Tsai et al.[16] Most prominent lines are a very broad line at 642 cm^{-1} assigned to torsional motion of the central −N−O− bond and a broad line at 1564 cm^{-1}assigned to the terminal N═O stretching frequency. On the basis of comparison with ab initio calculations, it was concluded that only the cis isomer is stable in aqueous solution. In a recent QM/MM simulation by LeBrero et al.,[23] the Raman line at 642 cm^{-1} was reassigned to a −NO− stretch, and it was shown how explicit inclusion of the aqueous solvent produced a significant red shift and broadening of this −NO− stretching frequency. Depending on the specific theoretical model used, they obtained a terminal N═O frequency in the range of 1475 to 1621 cm^{-1}. In conjunction with the calculated stabilities and the isomerization barrier,[31] it was again concluded that peroxynitrite in aqueous solution solely exists in the cis form. Additional information on *cis*- and *trans*-peroxynitrite can be obtained from low-temperature spectra of the species in an argon matrix,[22,24] where the terminal N═O vibrations of *cis*- and *trans*-peroxynitrite were observed close to 1460 and 1435 cm^{-1}, respectively. Therefore, in the majority of experimental and theoretical calculations, the terminal N═O vibration in *cis*-peroxynitrite is predicted to have the highest frequency. This is also in good agreement with our own calculations shown in Table 1. The values observed in the present work for *cis*- and *trans*-$ONOO^-$ are 1515 and 1580 cm^{-1}, which are in good agreement with the calculated values from Table 1 and in agreement with the Raman and infrared line position of the *cis*-$ONOO^-$ at 1564 cm^{-1} from Tsai et al.[16] As mentioned, there is a slight shift of the *cis*-$ONOO^-$ frequency when comparing the transient infrared spectrum in neutral solution with the steady-state infrared spectra observed in alkaline solutions by Tsai et al.[16] and in the present work. The simulations of Lebrero et al.,[23] Tsai et al.,[32] and our own calculations show that hydration predominantly takes place by hydrogen bonding to the peroxy oxygen atom ($ONOO^-\cdots H$), which results in a slightly shorter N═O bond and a correspondingly higher N═O vibrational frequency. We observe that the frequency is shifted from 1580 cm^{-1} in neutral solution to 1560 cm^{-1} when pH is increased. Assuming that peroxynitrite is

hydrated to a lesser degree at high pH, this is in accordance with the suggested hydration structures of the peroxynitrite−water system. A similar but opposite trend is seen in the infrared spectrum of nitrate. In this case, hydration leads to a red shift in the NO frequency as the water molecules on the average hydrogen bond equally to the oxygen atoms of nitrate, thus lengthening the NO bond slightly and lowering the vibrational frequency.

Cis and Trans Conversion. The photolysis of aqueous nitrate is initiated by the excitation of the $\pi \rightarrow \pi^*$ transition with a maximum near 205 nm. The strong transition accesses two nearly degenerate excited electronic states.[21] Resonance Raman experiments indicate that the excited states have pyramidal geometry[33] with a single longer NO bond compared with the ground state. Both of these properties facilitate the isomerization of nitrate into *trans*-peroxynitrite.

Only a few high-level ab initio calculations are available for the water−nitrate system, and they primarily address the solvent−solute interactions in the ground state. Simple geometric considerations suggest that the trans isomer of peroxynitrite is formed from the pyramidal geometry of the excited states in nitrate. However, experimental evidence[5,6,16] indicates that only the cis form is present in aqueous solution. This is in good agreement with ab initio calculations,[31] suggesting that the cis isomer is more stable by ∼20 kJ/mol with a rotational barrier of ∼100 kJ/mol around the ON−OO bond caused by the partially π-character of the planar peroxynitrite molecule. Our observation of *trans*-$ONOO^-$ immediately after the photolysis pulse is in accord with the notion of a pyramidal transition state, and the subsequent isomerization is also in agreement with the notion that the cis form is the more stable. We do, however, see only a partial isomerization, where about half of the trans isomerizes on a 25 ps time scale. This can be explained by considering the microenvironment in which the *trans*-$ONOO^-$ is formed: Nitrate is photolyzed by a 200 nm pulse, and a substantial amount of excess energy is dissipated to the solvent during the formation of $ONOO^-$. This excess energy rapidly (∼1 ps) thermalizes, resulting in a very hot solvent sphere surrounding the *trans*-$ONOO^-$ molecule. The local temperature increase causes the broadening and slight shift of the *trans*-$ONOO^-$ peak at 1515 cm^{-1} observed at short time delays. The hot solvent is also driving the isomerization of *trans*- into *cis*-$ONOO^-$, thereby converting about half of the *trans*- into *cis*-peroxynitrite. Simultaneously, the excess heat diffuses away from the reaction site, causing the temperature of the solvent sphere and, consequently, the rate of trans-to-cis isomerization to drop. Our experimental observations are limited to a delay time of 300 ps, and we do not observe a slow decay of the remaining *trans*-$ONOO^-$. However, the acceleration of the trans-to-cis isomerization caused by the heated solvent, estimated to be ∼30−60 degrees above room temperature[30] during the first tens of picoseconds, is in accordance with an isomerization barrier of ∼100 kJ/mol.

Observation of NO_2. In addition to the transient absorption pertaining to peroxynitrite, we also observe a relatively strong infrared peak at 1610 cm^{-1} that we tentatively assign to NO_2. On the basis of the observed and calculated line strength of the 1610 cm^{-1} vibration, we estimate that the yield of this third channel is between 15 and 25%. It is very interesting that the vibrational transition assigned to NO_2 appears with a large delay of ∼50 ps. We performed several experiments to test the validity of the assignment of the 1610 cm^{-1} peak to NO_2. We used different concentrations of nitrate and observed the 1610 cm^{-1} absorption to scale linearly with NO_3^- concentration. We photolyzed NO_3^- under acidic conditions (pH ∼1) and observed the rapid decay of the peroxynitrite peaks due to the formation of peroxynitrous acid (ONOOH), but the 1610 cm^{-1} was unaffected. Finally, we photodetached the electron in NO_2^-(aq) and observed NO_2 at 1610 cm^{-1}, again with a relatively slow appearance time similar to that observed in the photolysis of NO_3^-(aq). We can thus conclude that the signal at 1610 cm^{-1} is caused by NO_2 and is not associated with the formation and isomerization of peroxynitrite. To our knowledge, this is an unusually slow solvation process for NO_2, and one could instead speculate whether we are monitoring a slow dissociation of a solvent-separated contact pair $[O^-(aq)-NO_2]$. A similar solvent-separated contact pair was recently shown in simulations[34] to play a role in the homolysis of the peroxynitrous acid (ONOOH) into OH + NO_2. If this assignment is valid, then our results thus provide a direct measurement of the lifetime of the solvent-separated contact pair. The observed lifetime is, based on the risetime of the 1610 cm^{-1}, ∼50 ps. This relatively long lifetime indicates that the contact pair must be considered to be an important intermediate in secondary reactions following the photolysis of concentrated nitrate solution. In particular, when the solvent-separated contact pair breaks up, the O^- moiety will be protonated (pH ∼7) and thus serve as a source of hydroxyl radicals. Furthermore, experimental and theoretical studies are underway to confirm the assignment of the 1610 cm^{-1} peak to NO_2. The slow appearance of the NO_2 signal is also the reason we did not observe it in our previous UV pump−UV/vis probe experiments.[5] In that work, we scanned only to delays shorter than 18 ps at selected wavelengths not including the region where NO_2 absorbs. Furthermore, given the very low UV extinction coefficient of NO_2(aq), the estimated signal strengths would be close to the detection limit. Given the observation of a slowly emerging NO_2 signal in this work, we reconsider the assignment and yield of the third channel in eq 1. The third channel was assigned to $[NO + O_2]^-$, but with the present observation, we find that both the UV and IR transient data are consistently described by $[NO_2 + O^-]$. The UV spectra of O_2^-, NO^-, and O^- are very similar apart from their extinction coefficient. The smaller extinction coefficient of O^- in UV and the strength of the 1610 cm^{-1} line observed in this work led us to increase the yield of the third channel from 8 to 15−25%. We also note that reassigning the third channel to $NO_2 + O^-$ is in agreement with recent work from Goldstein and Rabani.[6] We have considered if the solvent separated contact pair of $[NO_2+O^-]$ could be formed from *trans*-peroxynitrite along with *cis*-peroxynitrite. However, because of the low signal strengths and the inherent problem of the large background signal caused by the heated water solvent, we are not able to answer this question presently.

Conclusions

We have observed the formation of *trans*-$ONOO^-$ following the photolysis of NO_3^- in D_2O solution at 200 nm. Using infrared probe frequencies, we observed the trans isomer at 1515 cm^{-1} and subsequently its partial isomerization to the *cis*-isomer on a 25 ps time scale. After 25 ps, the ratio between *cis*- and *trans*-$ONOO^-$ is unchanged out to the longest delay (300 ps) observed in this work. The *cis*-$ONOO^-$ is observed at 1580 cm^{-1}, which is in good agreement with infrared and Raman experiments.[16] We have also observed a prominent infrared absorption at 1610 cm^{-1}, which is assigned to NO_2 following the slow (∼50 ps) decay of a solvent-separated contact pair between O^- and NO_2.

Acknowledgment. We acknowledge the support from the Danish Natural Science Research Council and the Carlsberg

Foundation. We wish to thank Professor Koppenol and his colleagues at ETH, Zürich, for useful discussions.

Supporting Information Available: Complete ref 18. This material is available free of charge via the Internet at http://pubs.acs.org.

References and Notes

(1) The recommended IUPAC name for peroxynitrite is oxoperoxonitrate(1-), and one should also use syn and anti in place of cis and trans. We, however, chose to use the *cis*- and *trans*-peroxynitrite names commonly accepted in the literature.

(2) Mack, J.; Bolton, J. R. *J. Photochem. Photobiol., A* **1999**, *128*, 1.

(3) Mark, G.; Korth, H.-G.; Schuchmann, H.-P.; von Sonntag, C. *J. Photochem. Photobiol., A* **1996**, *101*, 89.

(4) Keiding, S. R.; Madsen, D.; Larsen, J.; Jensen, S. K.; Thøgersen, J. *Chem. Phys. Lett.* **2004**, *390*, 94.

(5) Madsen, D.; Larsen, J.; Jensen, S. K.; Keiding, S. R.; Thogersen, J. *J. Am. Chem. Soc.* **2003**, *125*, 15571.

(6) Goldstein, S.; Rabani, J. *J. Am. Chem. Soc.* **2007**, *129*, 10597.

(7) Shuali, U.; Ottoleng, M.; Rabani, J.; Yelin, Z. *J. Phys. Chem.* **1969**, *73*, 3445.

(8) Bianco, R.; Wang, S. Z.; Hynes, J. T. *J. Phys.Chem. A* **2008**, *112*, 9467.

(9) Løgager, T.; Sehested, K. *J. Phys. Chem.* **1993**, *97*, 6664.

(10) Hodges, G. R.; Ingold, K. U. *J. Am. Chem. Soc.* **1999**, *121*, 10695.

(11) Beckman, J. S.; Beckman, T. W.; Chen, J.; Marshall, P. A.; Freeman, B. A. *Proc. Natl. Acad. Sci. U.S.A.* **1990**, *87*, 1620.

(12) Beckman, J. S.; Koppenol, W. H. *Am. J. Physiol.: Cell Physiol.* **1996**, *271*, C1424.

(13) Kissner, R.; Nauser, T.; Bugnon, P.; Lye, P. G.; Koppenol, W. H. *Chem. Res. Toxicol.* **1997**, *10*, 1285.

(14) Merenyi, G.; Lind, J.; Goldstein, S.; Czapski, G. *J. Phys. Chem. A* **1999**, *103*, 5685.

(15) Goldstein, S.; Lind, J.; Merenyi, G. *Chem. Rev.* **2005**, *105*, 2457.

(16) Tsai, J. H. M.; Harrison, J. G.; Martin, J. C.; Hamilton, T. P.; Vanderwoerd, M.; Jablonsky, M. J.; Beckman, J. S. *J. Am. Chem. Soc.* **1994**, *116*, 4115.

(17) Tauber, M. J.; Mathies, R. A.; Chen, X. Y.; Bradforth, S. E. *Rev. Sci. Instrum.* **2003**, *74*, 4958.

(18) Frisch, M. J.; et al. *Gaussian 03*, revision C.02; Gaussian, Inc.: Wallingford, CT, 2004.

(19) Cramers, C. J. *Essentials of Computational Chemistry*, 2nd ed.; Wiley: Chichester, U.K., 2004.

(20) Ramesh, S. G.; Re, S. Y.; Hynes, J. T. *J. Phys. Chem. A* **2008**, *112*, 3391.

(21) Waterland, M. R.; Stockwell, D.; Kelley, A. M. *J. Chem. Phys.* **2001**, *114*, 6249.

(22) Liang, B. Y.; Andrews, L. *J. Am. Chem. Soc.* **2001**, *123*, 9848.

(23) Lebrero, M. C. G.; Perissinotti, L. L.; Estrin, D. A. *J. Phys. Chem. A* **2005**, *109*, 9598.

(24) Relph, R. A.; Bopp, J. C.; Johnson, M. A.; Viggiano, A. A. *J. Chem. Phys.* **2008**, *129*, 64305.

(25) Lo, W. J.; Lee, Y. P.; Tsai, J. H.; Tsai, H. H.; Hamilton, T. P.; Harrison, J. G.; Beckman, J. S. *J. Chem. Phys.* **1995**, *103*, 4026.

(26) Lo, W. J.; Lee, Y. P.; Tsai, J. H. M.; Beckman, J. S. *Chem. Phys. Lett.* **1995**, *242*, 147.

(27) Robinson, K. M.; Beckman, J. S. *Methods Enzymol.* **2005**, *396*, 207.

(28) Martinez, G. R.; Di Mascio, P.; Bonini, M. G.; Augusto, O.; Briviba, K.; Sies, H.; Maurer, P.; Rothlisberger, U.; Herold, S.; Koppenol, W. H. *Proc. Natl. Acad. Sci. U.S.A.* **2000**, *97*, 10307.

(29) Ashihara, S.; Huse, N.; Espagne, A.; Nibbering, E. T. J.; Elsaesser, T. J. *J. Phys. Chem. A* **2007**, *111*, 743.

(30) Petersen, C.; Thøgersen, J.; Jensen, S. K.; Keiding, S. R.; Sassi, P. *Phys. Chem. Chem. Phys.* **2008**, *10*, 990.

(31) Tsai, H. H.; Hamilton, T. P.; Tsai, J. H.; van der Woerd, M.; Harrison, J. G.; Jablonsky, M. J.; Beckman, J. S.; Koppenol, W. H. *J. Phys. Chem.* **1996**, *100*, 15087.

(32) Tsai, H. H.; Hamilton, T. P.; Tsai, J. H. M.; Beckman, J. S. *Struct. Chem.* **1995**, *6*, 323.

(33) Waterland, M. R.; Kelley, A. M. *J. Chem. Phys.* **2000**, *113*, 6760.

(34) Gunaydin, H.; Houk, K. N. *J. Am. Chem. Soc.* **2008**, *130*, 10036.

JP906354C